

MEMORY AUGMENTED OPTIMIZERS FOR DEEP LEARNING

Paul-Aymeric McRae ^{†1}, Prasanna Parthasarathi ^{†1,2}, Mahmoud Assran^{1,2}, and Sarath Chandar^{1,3,4}

¹Mila - Quebec AI Institute, Canada

²McGill University, Canada

³École Polytechnique de Montréal, Canada

⁴Canada CIFAR AI Chair

ABSTRACT

Popular approaches for minimizing loss in data-driven learning often involve an abstraction or an explicit retention of the history of gradients for efficient parameter updates. The aggregated history of gradients nudges the parameter updates in the right direction even when the gradients at any given step are not informative. Although the history of gradients summarized in meta-parameters or explicitly stored in memory has been shown effective in theory and practice, the question of whether *all* or only a subset of the gradients in the history are sufficient in deciding the parameter updates remains unanswered. In this paper, we propose a framework of memory-augmented gradient descent optimizers that retain a limited view of their gradient history in their internal memory. Such optimizers scale well to large real-life datasets, and our experiments show that the memory augmented extensions of standard optimizers enjoy accelerated convergence and improved performance on a majority of computer vision and language tasks that we considered. Additionally, we prove that the proposed class of optimizers with fixed-size memory converge under assumptions of strong convexity, regardless of which gradients are selected or how they are linearly combined to form the update step.

1 INTRODUCTION

Gradient-based learning involves minimizing a scalar-valued function $F(\theta)$ with respect to a parameter vector $\theta \in \mathbb{R}^d$ using an iterative procedure. When training over n examples of input-output pairs, (x_i, y_i) , the optimization problem boils down to solving $\min_{\theta} F(\theta)$, where

$$F(\theta) = \frac{1}{n} \sum_{i=1}^n L_i(\theta), \quad \text{with} \quad L_i(\theta) = \mathcal{L}(M_{\theta}(\mathbf{x}_i), y_i),$$

for some problem-dependent loss function \mathcal{L} and a predictive model M parameterized by θ .

Stochastic Gradient Descent (SGD) (Robbins and Monro, 1951) is one common method used to tackle this problem, and is often preferred to full-batch Gradient Descent when the quantity of data required to train θ is large, since it can be more efficient to measure a single component of the gradient (or a mini-batch of gradients (Bottou, 1999)), and move in a noisy direction, than to compute a full gradient at each time step. Several techniques have been proposed to further accelerate the convergence of SGD (Ghadimi and Lan, 2016; Allen-Zhu and Yuan, 2016; Zhou et al., 2018). These include approaches that maintain a knowledge of previous gradients implicitly by summarizing them in a momentum buffer (Polyak, 1964b), and potentially adapting the learning rate based on the gradient statistics (Duchi et al., 2011; Hinton et al., 2012; Zeiler, 2012; Kingma and Ba, 2015).

Optimization techniques such as SGD with Momentum (Polyak, 1964a), AdaGrad (Duchi et al., 2011), RMSprop (Hinton et al., 2012), AdaDelta (Zeiler, 2012), and Adam (Kingma and Ba, 2015) maintain a set of buffers that track running moments of the gradients. Such light-weight techniques

[†]The two authors contributed equally to this paper.

have shown significant application advantage in practice, whereas in theory, algorithms that store all of the gradients, like SAG (Roux et al., 2012) and SAGA (Defazio et al., 2014), can achieve better convergence. A drawback of full-history methods is that the memory requirement linearly increases with the size of the data.



Figure 1: Common optimization algorithms placed over the spectrum of memory requirements. The proposed algorithms the C variants have a fixed sized memory to store gradients during training.

The spectrum of gradient-based approaches (Figure 1) that use a knowledge of the past gradients has Adam, RMSprop and SGD with Momentum on the one end and approaches like SAG and SAGA on the other. An optimization algorithm in the middle of this spectrum can use less memory than full-history methods while providing richer updates than adaptive-gradient methods.

Limited-Memory BFGS (Nocedal, 1980) and its online, stochastic form, oLBFGS (Schraudolph et al., 2007) aim to exploit this trade-off, but may not converge faster than SGD (Mokhtari et al., 2015), and are thus disadvantaged compared to accelerated SGD variants. As a stepping stone towards reaping the advantages of both ends of

the spectrum, we propose using memory to augment conventional optimizers. This memory is used to store a small set of *critical gradients* (e.g., gradients with a larger ℓ_2 -norm) that are occasionally updated with newer gradients. Specifically, rather than storing gradients for all the examples in the dataset, our proposed approach aims to find a smaller set of gradients to store that will aid in the optimization process. Through extensive experiments we show that this marginal increase in the memory requirement (Figure 1) provides accelerated convergence and even improved test performances in majority of the experiments.

In this work, we:

- Present a framework of memory-augmented optimizers compatible with popular gradient-based algorithms.
- Prove theoretically that such algorithms converge for smooth strongly convex objectives.
- Show that the proposed memory augmented optimizers can lead to faster convergence and better final performance through exhaustive empirical study on eight different architectures among four different tasks (classification, language modeling, natural language inference, and dialogue) and six different datasets.
- Demonstrate the memory augmented optimizers’ robustness to gradient selection, replacement, or the aggregation techniques to summarize information in the memory.

2 MEMORY-AUGMENTED OPTIMIZERS

In this work, we propose augmenting standard optimizers with a fixed size memory of past gradients. The gradients are stored in the limited memory only when they are deemed *critical* as defined by their ℓ_2 -norm.

Gradient Selection to the Memory Letting $g_t := \nabla_{\theta} L_i(\theta_t)$ denote a component (or mini-batch) gradient at time-step t , we use $\|g_t\|_2$ as a scalar indicator of the importance of the gradient, which serves as a proxy for the priority of a gradient to remain in the memory buffer g_c . In order to ensure that the buffer eventually flushes out stale gradients, the proxy norms for gradients in the buffer are scaled down by a hyperparameter decay factor, denoted $\text{decay} \in [0, 1)$.

The proposed approach maintains a gradient buffer of fixed capacity C and stores the gradients selected by a chosen heuristic. We refer our heuristic as the *critical gradients*, which stores the *top C* gradients by using the ℓ_2 -norm of g_t to determine priority. Gradients in the buffer are stored as tuples $(\|g_t\|_2, g_t)$, akin to a key-value pair in a dictionary structure, where the key $\|g_t\|_2$ is referred to as the proxy norm, and decayed at each time step t by a decay factor $\text{decay} \in [0, 1)$. At any iteration t during training, the gradient in a full capacity priority buffer with the smallest ℓ_2 proxy-norm is

replaced by the current mini-batch gradient g_t if $\|g_t\|_2$ is greater than the smallest ℓ_2 proxy-norm in the buffer. The multiplicative `decay` factor ensures that the buffer is frequently refreshed with more recent gradients. Note that only the proxy-norm used for the heuristic rule is decayed by the decay factor `decay` $\in [0, 1)$, while the gradient itself is not affected. This technique of storing the critical gradients is general enough to be employed in any deep learning model, and can be easily be combined with many existing adaptive gradient optimization algorithms, such as those described in (Polyak, 1964b; Zeiler, 2012; Duchi et al., 2011; Hinton et al., 2012; Kingma and Ba, 2015).

Critical Gradient Stochastic Gradient Descent Critical Gradient Stochastic Gradient Descent (SGD_C) is the explicit integration of critical gradients into SGD. Specifically, the iteration comes as,

$$\theta_{t+1} = \theta_t - \alpha \cdot \text{aggr}(g_t, \mathbf{g}_c), \quad (1)$$

where \mathbf{g}_c is the set of critical gradients and `aggr` denotes an aggregation function which is used to combine the critical gradients with the current-iteration gradient. We propose two possible functions for `aggr` including `mean`, the average of g_t and all critical gradients, and `sum`, the addition of g_t to the average of all critical gradients. Mathematically, for a buffer of size C these are defined as

$$\text{mean}(g_t, \mathbf{g}_c) = \frac{1}{C+1}(g_t + \sum_{g_c \in \mathbf{g}_c} g_c) \quad (2) \quad \text{sum}(g_t, \mathbf{g}_c) = g_t + \frac{1}{C} \sum_{g_c \in \mathbf{g}_c} g_c \quad (3)$$

In general, we find optimization to be robust to the specific choice of aggregation function, but we do observe that adaptive learning rate methods (Adam, RMSprop) perform best with `mean`, while conventional SGD (with or without Polyak momentum) performs best with `sum`.

Critical Gradients with Accelerated Methods Agarwal et al. (2019) show that curvature in adaptive gradients can be estimated without loss of generality with a finite moving window of past gradients. Following which we propose critical gradient extensions of SGD with Momentum (SGDM) (Eq.4), RMSprop (Eq.5), and Adam (Eq.6). The retention of the critical gradients can be naturally extended to more first-order optimization methods with the replacement of g_t in those algorithms with `aggr` (g_t, \mathbf{g}_c). The update steps for the corresponding C versions are as follows:

$\begin{aligned} m_t &= \gamma \cdot m_{t-1} + \text{aggr}(g_t, \mathbf{g}_c) \\ \theta_{t+1} &= \theta_t - \alpha \cdot m_t \end{aligned} \quad (4)$	$\begin{aligned} m_t &= \beta_1 m_{t-1} + (1 - \beta_1) \cdot \text{aggr}(g_t, \mathbf{g}_c) \\ v_t &= \beta_2 v_{t-1} + (1 - \beta_2) \cdot (\text{aggr}(g_t, \mathbf{g}_c))^2 \\ \hat{m}_t &= \frac{m_t}{1 - \beta_1^t} \\ \hat{v}_t &= \frac{v_t}{1 - \beta_2^t} \\ \theta_{t+1} &= \theta_t - \frac{\eta}{\sqrt{\hat{v}_t} + \epsilon} \hat{m}_t \end{aligned} \quad (6)$
$\begin{aligned} \mathbb{E}[g^2]_t &= 0.9 \cdot \mathbb{E}[g^2]_{t-1} + 0.1 \cdot \text{aggr}(g_t, \mathbf{g}_c)^2 \\ \theta_{t+1} &= \theta_t - \frac{\eta}{\sqrt{\mathbb{E}[g^2]_t} + \epsilon} \cdot \text{aggr}(g_t, \mathbf{g}_c) \end{aligned} \quad (5)$	

The general algorithm to integrate critical gradients into any optimizer is provided in Algorithm 1 in Appendix A. Replacing g_t with `aggr` allows the optimization function to retain key gradients and optimize the parameters. The acceleration provided by the `topC` gradients complements the adaptive learning rate methods by not only computing the learning rate with respect to g_t but also with respect to the critical gradients from the past. We observe that all C -extended optimizers in our experiments in § 5 lead to faster convergence than their vanilla, non memory-augmented counterparts.

3 PROOF OF CONVERGENCE

Consider the SGD_C update in Equation (1), where `aggr` (g_t, \mathbf{g}_c) outputs a linear combination of the critical gradients in memory $g_k \in \mathbf{g}_c$, and the stochastic gradient g_t , which is computed at the current parameters θ_t . When the staleness of gradients in the memory is bounded, we can prove convergence of this method through the lens of *linear multi-step methods*. Formally, suppose there exists an integer

$K > 0$ such that $g_k \in \mathcal{g}_c$ at iteration t , implies $t - k < K$, and suppose the objective $F : \mathbb{R}^d \rightarrow \mathbb{R}$ is twice-continuously differentiable, L -smooth, and μ -strongly convex, with $0 < \mu \leq L$. Assume that for all k , the stochastic gradient g_k is a random vector satisfying

$$\mathbb{E}[g_k] = \nabla f(\theta_k) \quad \text{and} \quad \mathbb{E} \left[\|g_k - \nabla f(\theta_k)\|^2 \right] \leq \sigma^2,$$

for some finite constant σ^2 . Letting $\zeta_k := g_k - \nabla f(\theta_k)$ denote the gradient noise at iteration k , we take these gradient noise terms to be mutually independent. For examples of functions satisfying these properties, see, e.g., (Nesterov, 2004; Bubeck, 2015). Examples of typical tasks satisfying these assumptions are ℓ_2 -regularized logistic regression and ℓ_2 -regularized least-squares regression. Taken together, these properties imply that the Hessian $\nabla^2 F(\theta)$ exists, and for all $\theta \in \mathbb{R}^d$, the eigenvalues of $\nabla^2 F(\theta)$ lie in the interval $[\mu, L]$. In this case, let θ^* denote the unique minimizer of F .

To prove convergence, we view SGD_C as a linear multi-step method, i.e., the parameters at the current time step are updated with a linear combination of gradients from the past K time steps. From this view, we can describe the evolution of the algorithm according to a discrete-time linear dynamical system, the convergence of which is characterized by the spectral properties of the system matrix. Our convergence theorem relies on the largest singular value of this system matrix, but can be strengthened to instead rely on the spectral radius of the system matrix by constructing an appropriate Lyapunov function containing a time-invariant system matrix satisfying a particular Integral Quadratic Constraint (IQC) (Lessard et al., 2016). However, one downside of the IQC framework is that one must typically solve a semidefinite program to obtain explicit convergence rates (Hu and Lessard, 2017), whereas Theorem 1 (refer Appendix §B for proof) provides an analytical convergence rate.

Theorem 1 (Linear Convergence of SGD_C). Let

$$q_{(\alpha, K)} := \sup_{\{w_k \in [0, 1], \{\eta_k \in [\mu, L]\}} \rho(\Lambda),$$

where $\rho(\Lambda)$ are the singular values of the numerical matrix

$$\Lambda := \begin{bmatrix} \lambda_0 & \lambda_1 & \cdots & \lambda_{K-1} \\ 0 & 1 & \cdots & 0 \\ \cdots & \cdots & \cdots & \cdots \\ 0 & 0 & \cdots & 1 \end{bmatrix} \in \mathbb{R}^{K \times K},$$

with $\lambda_0 = 1 - \alpha\eta_0$ and $\lambda_k = -\alpha w_k \eta_k$ for $k > 0$. If the step-size $\alpha > 0$ is chosen sufficiently small, such that $q_{(\alpha, K)} < 1$, then

$$\mathbb{E} \|\theta_{t+1} - \theta^*\|^2 \leq q_{(\alpha, K)}^{2t} \|\theta_1 - \theta^*\|^2 + \frac{\alpha^2 K}{1 - q_{(\alpha, K)}^2} \sigma^2,$$

where the expectation on the left hand side is with respect to the joint distribution over the random noise variables ζ_k, \dots, ζ_1 .

Theorem 1 shows that SGD_C can be made to converge exponentially fast to a neighbourhood of the solution, the size of which is proportional to the variance of the stochastic gradients σ^2 and the step-size α^2 . If $K = 1$ (i.e., the memory \mathcal{g}_c , at all times t , only contains the mostly recently computed gradient), then SGD_C reduces to regular stochastic gradient descent, and the rate $q_{(\alpha, K)}$ in Theorem 1 reduces to the well known convergence rate of SGD for smooth strongly convex functions ($\max_{\eta \in [\mu, L]} |1 - \alpha\eta L|$), and the variance bound reduces to the standard variance bound for SGD with a constant step-size ($\alpha^2 \sigma^2 / (1 - q^2)$), see, e.g., (Bottou et al., 2018; Assran and Rabbat, 2020). For $K > 1$, it may be possible to choose the step-size α and the aggregation weights $\{w_k\}$ to obtain accelerated convergence rates, faster than SGD. For example, accelerated gradient methods such as Polyak and Nesterov momentum can be viewed as multi-step methods with $K = 2$. Note that although K appears in the numerator of the coefficient of the variance term, it is also present in the rate term in the denominator, where faster convergence rates, smaller $q_{(\alpha, K)}$, directly lead to smaller variance bounds. Note that expressing the convergence rate of a multi-step method as the roots of a polynomial, as we do in Theorem 1, is not new; see, e.g., Polyak (1964a).

4 RELATED WORK

Past-Gradients-Summarizing Optimizers Several popular optimization algorithms incorporate the history of previous gradients through a summarizing variable. In practice, this is often done by

means of a decaying average, which is updated with each iteration. SGD with Momentum (SGDM) (Polyak, 1964b) uses this summary variable as a means of stabilizing descent along one path even if the current gradient points are uninformative. A variant of SGDM uses Nesterov momentum (NAG) (Nesterov, 1983; Sutskever et al., 2013) and applies the velocity to the current gradient as a correction factor. SGD_C shares similarity with NAG except in SGD_C the “momentum” is computed only using C selected gradients. In a different use of a summarizing variable, AdaGrad (Duchi et al., 2011) keeps a running sum of *squared* gradients which is used to dynamically adjust the learning rate. AdaDelta (Zeiler, 2012) and RMSprop (Hinton et al., 2012) replace AdaGrad’s running sum with a decaying average of the squared gradients. Adam (and AdaMax) (Kingma and Ba, 2015) uses a combination of momentum and a decaying-average-dependent learning rate. In general, the C variants (SGD_C , Adam_C , RMSprop_C , SGDM_C) provide an additional “layer” to the base algorithms that ensures any parameter computed within the algorithm incorporates the critical gradients. Although optimization using a fixed size buffer has been in existence, the novelty of the C variants comes from adding a heuristic to keep only the gradients that provide the largest displacements towards the minimum.

Memory-Enhanced Optimizers Our algorithm belongs to a class of optimization methods which are aware of a limited history of gradients from previous iterations. One fellow algorithm from this class is Limited-History BFGS (LBFGS) (Nocedal, 1980), an optimization technique which approximates the Hessian of a function using a limited history of gradients, then uses the estimated Hessian to compute the descent direction for optimization. An online version of LBFGS (oLBFGS), well-suited for a machine learning context, was proposed by Schraudolph et al. (2007). These LBFGS methods utilize a moving window of past gradients, rather than our idea to maintain “critical” gradients based on a well-defined metric.

The storage of past gradients as a means to improve optimizer convergence is not a novel idea; both Stochastic Accelerated Gradient (SAG) (Roux et al., 2012) and SAGA (Defazio et al., 2014) do so in the context of accelerating stochastic gradient descent, while Stochastic Dual Coordinate Ascent (Shalev-Shwartz and Zhang, 2013) uses previous gradients for coordinate ascent. Empirically and theoretically, these techniques have been shown to yield good performance. The SAG and SAGA algorithms differ in their weight update step, but both involve storage of up to n gradients, where n is the number of training examples, which can be costly. Our method relies on the storage of a fixed number of gradients and uses a heuristic to decide whether to store a gradient in a dataset-size-independent memory. Our class of optimizers can natively run in a batch-based training loop unlike originally presented SAG and SAGA. Gazagnadou et al. (2019) address this issue in their recent work. We also extend our method beyond SGD to several other first-order optimization methods.

SAG and SAGA belong to the family of variance-reduced gradient-based algorithms (J. Reddi et al., 2015). Such algorithms theoretically and empirically outperform SGD, though with the trade-off of having a large cost in terms of memory or gradient evaluations. Some algorithms in this framework attempt to bridge both costs, for instance a variant of Stochastic Variance Reduced Gradient (SVRG) (Johnson and Zhang, 2013) stores intermediate gradients to avoid recomputing them later, and StochAstic Recursive grAdient algoritHm (SARAH) (Nguyen et al., 2017) uses a summarizing variable. Our method attempts to recapture the benefits of variance-reduced methods without significant computation or memory overhead.

Optimizing Optimizers Our optimizer method also shares similarities with techniques which seek to optimize optimizers; that is, techniques which automatically learn the best way to accomplish the task of tuning the optimizer used in an outer-problem. The architecture proposed by Metz et al. (2020) uses an LSTM per tensor of the network parameters, with each LSTM being passed the gradient norms to influence the parameter update step, echoing our technique’s use of gradient norm as a critical metric to parameter updates. In a similar vein, Andrychowicz et al. (2016) also use LSTMs, which are fed the complete gradient, and use the LSTM’s recurrence as a means of implicitly accessing past gradients. Li and Malik (2017) uses a reinforcement learning-based approach and defines a state-space which includes a recent history of gradients. While our method equally maintains a ledger of past gradients, unlike this latter approach we use ℓ_2 -norm as a metric to pick out the critical gradients instead of arbitrarily keeping a recent history.

Motivation for explicit memory Motivation for explicit memory-augmented optimizers over the ones that maintain an implicit summarization of history comes from memory-augmented neural

seed values— Adam, SGD, SGDM, RMSprop, Adam_C, SGD_C, SGDM_C, and RMSprop_C on 9 tasks — CIFAR100, CIFAR10, SNLI-I, SNLI-C, SNLI-BL, MWoZ-RoB, MWoZ-BL, PTB-LS, and WIKITEXT-LS*. For a fair comparison, we follow the standard experimental protocol for all the experiments and tune all the hyperparameters of an optimizer individually for every task.

Our experimental results are aggregated from 5 independent runs, with the hyperparameters for each optimizer extensively tuned. This involves tuning the learning rate in all optimizers, the topC and decay parameters in all C algorithms, and all optimizer-specific hyperparameters in both the vanilla versions and their C counterparts. A full description of the values used to tune the various parameters, architecture and dataset details are in Appendix §E, §D, and §C respectively. The best set of hyperparameters was selected based on which ones yielded the best validation performance (i.e. highest accuracy, highest BLEU score, or lowest perplexity).

Figure 2(a) shows that the proposed C variants provided a consistent acceleration in convergence over their vanilla versions. The accelerated convergence also resulted in improved test performance, as highlighted in Figure 2(b) (Exhaustive list is provided in Appendix §G). In addition to the aforementioned improvements in vanilla-vs- C comparisons, the C optimizers yielded the best test performance across all 8 optimizers in 6/9 tasks. Of the three remaining tasks, the C versions performed close to the vanilla versions. In the case of MWoZ – BL RMSprop_C the C version showed marginally accelerated convergence close to the optimal solution. Furthermore, Figure 3 compares the validation performance after each epoch when trained with the different optimizers on the different tasks. One immediate observation was that in language experiments – SNLI, PTB, MWoZ – the C versions stayed above most if not all of the vanilla optimizers. While that separation is not as clear in the vision tasks, we observed that the pairwise comparison mostly put the C optimizer at an advantage in accelerated convergence.

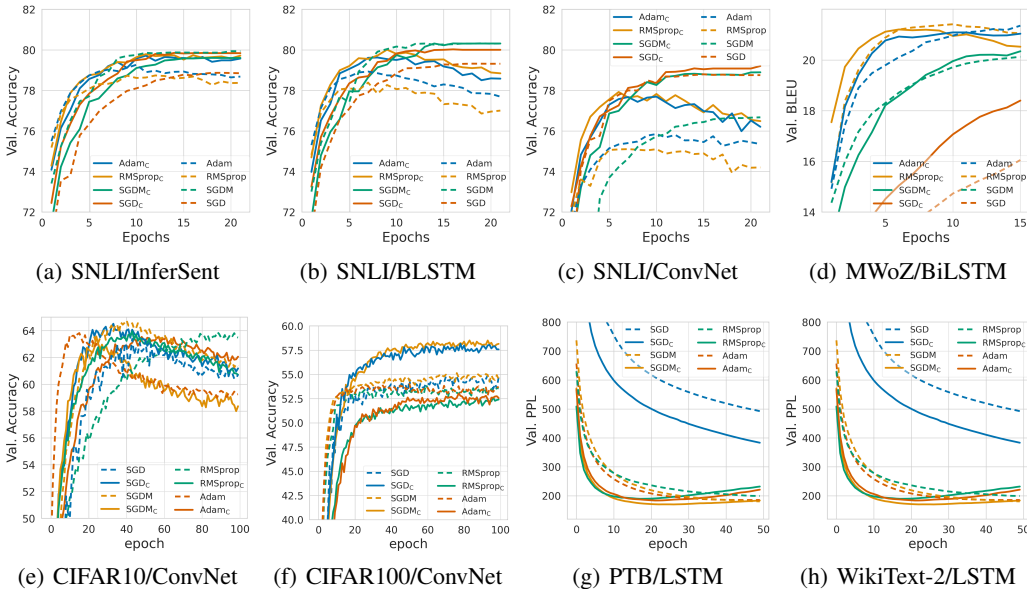


Figure 3: The validation performance comparison of the proposed optimizers and their vanilla versions showed that, in general, the proposed optimizers showed accelerated convergence than their counterparts. Also, in the 3 tasks — SNLI-I (a), SNLI-BL (b) and MWoZ-BL (d) where the C methods are not the optimal — only falls short by a negligible margin. For ease of visualization, confidence intervals across seeds are suppressed.

*Code to reproduce results: <https://github.com/chandar-lab/CriticalGradientOptimization>.
 Optimizer package: <https://github.com/chandar-lab/CGOptimizer>

6 ANALYSIS

Buffer Staleness Bound A key assumption behind the theoretical convergence of SGD_C is the existence of an upper bound on the buffer gradients’ staleness (i.e the number of iterations a gradient remains in the critical buffer). We analysed the distribution of average number of steps a gradient stays in the memory for the different values of top_C and decay in Figure 4. We observe that tuning the parameters ensures that gradients in the buffer are refreshed frequently, allowing for a renewal of information. Later, in analysing the effect of decay and top_C on the performance in a task, we observe that the higher performance of the C methods correlate with the findings of this analysis.

Use of Critical Gradients Our Critical Gradient method utilizes a buffer which is filled by using a norm-based, “King of the Hill” sampling of incoming gradients, i.e. gradients always stored and sorted in decreasing order by ℓ_2 -norm, with the smallest norm always being the one removed. We conduct ablation studies to probe the three assumptions of critical gradients using LSTM architecture with PTB dataset.: (a) the use of norm as a controlling metric, (b) the removal of the smallest-norm entry when adding to a full buffer, and (c) the update step depending on an ensemble of buffer gradients via the mean rather than on select gradients.

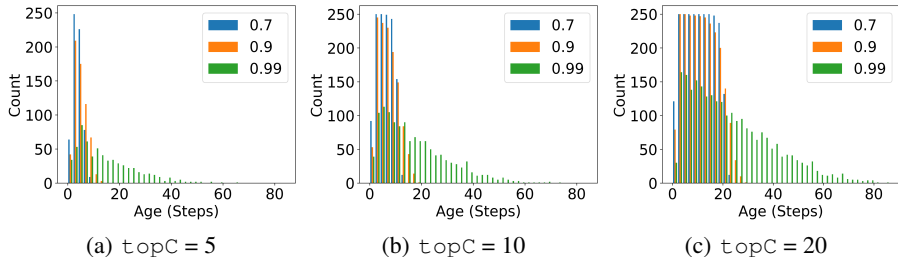


Figure 4: Histograms showing ages of the buffer as recorded at the end of every epoch, across five seeds for several decay values, for a MLP on MNIST. 0.99 decays at a much slower rate, keeping stale gradients in the memory, while 0.7 replaces the gradients frequently. Also, the size of the buffer (top_C), as expected, correlates directly with retention of stale gradients.

Addressing assumption (a) we test the use of maximal norm sampling (Figure 5(a)) by comparing with Cosine Similarity Sampling (CSS), Cosine Diversity Sampling (CDS), Mean-Norm Diversity Sampling (MNDS), and random sampling via "coin toss". Figure 5(b) depicts our algorithm alongside different gradient replacement methods, including Random Replacement (RR) and Norm-Controlled Probabilistic Replacement (NCPR), as well as comparing against keeping a running First-In-Fist-Out (FIFO) queue and only using the smallest ("bottomC") gradients. Finally we compare the typical optimizer aggregation method with the buffer gradients minimum, maximum, and median norm (Figure 5(c)). A full description of these techniques can be found in Appendix §F.9.

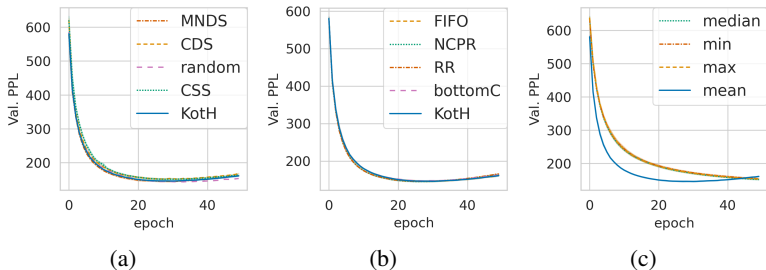


Figure 5: (a) compares gradient selection techniques based on different metrics, (b) compares different replacement strategies when flushing out a gradient from memory and (c) compares choice of aggregating the gradients in the buffer. The algorithm converges in all the different choices.

We observe in most cases, the sampling (a) and replacement (b) strategies for gradients in the buffer and all ablations converge regardless of these considerations. While the Critical Gradients formulation is not unique as a high-performing implementation of a memory-augmented optimizer, it remains conceptually straightforward, easy to implement, and the buffer properties are deterministic as compared to some of our ablation studies which were probabilistic. Although, a rigorous analysis is necessary to verify the generality of this result.

Experiments comparing the performance of mean-based aggregation against aggregation based on individual gradients show that aggregation based on the ensemble must be employed, and that the optimizers benefit from the added information.

Effect of hyperparameters We study the performance’s sensitivity to `decay` and `topC` using `AdamC` on different tasks.

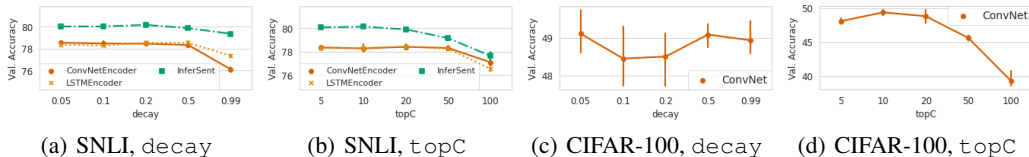


Figure 6: We observe that non-trivial choices of `decay` and `topC` provided best performance for `AdamC` with different architectures on SNLI task. Also, the usefulness of explicit memory aligns with the evidence on gradient staleness from Figure 4.

The `decay` $\in [0, 1)$ parameter allows to tune the retention of critical gradient information from the past. Setting `decay` = 0 reduces the priority of new gradients added to the buffer, making the C variants behave like an average over a moving window of length `topC`. On the other extreme, `decay` = 1 does not decrease the priorities of the past gradients and allows them to be in the buffer for a much longer period hindering the convergence of the optimizers. Also, `decay` maintains the staleness of the gradients by exponentially decaying their priority in the memory buffer. We experimented with `AdamC` optimizer for the different values of `decay` with every other parameter fixed (Figure 6). We observed that `decay` values closer to 1 did not have any advantage at best or leads to inferior performance on an unseen set at worst in most of the tasks.

`topC` $\in [0, \infty)$ defines the size of the buffer that holds the past gradients. When `topC` is set to 0, C variants behave like the base algorithms and when `topC` is the size of the dataset, the optimizer becomes SAG-like. Also, `topC` is directly proportional to the staleness of the gradients in the buffer. A higher `topC`, though, guarantees better expressibility also becomes responsible for more stale gradients in the buffer. Bengio et al. (2020) also observes a similar issue in momentum used in TD-learning and proposes a correction factor to alleviate the issue. Here, the staleness is contained with the parameters `topC` and `decay`. As an empirical evidence, we observe that the optimizers perform well on the validation set with lower `topC` values. In most of the experiments, `topC` > 20 was either not useful or was hurting the performance (also in Appendix F).

7 CONCLUSION

We propose a general method to enhance the performance of an optimizer with an augmented memory buffer to maintain a limited set of critical gradients from the history. The proposed memory mechanism, when integrated with several state-of-the-art optimizers, accelerated the learning in all cases and also improved their performance in several cases. The C family of optimizers proposed in this paper are the first steps towards designing smart optimizers that can learn to optimize. Some of the immediate future research directions include learning *what* to store in the memory and learning *how* to integrate the information in memory to the gradient update steps.

Acknowledgements We would like to acknowledge Compute Canada and Calcul Quebec for providing computing resources used in this work. The authors would also like to thank members of Chandar Research Lab, Mila for helping with the code reviews and reviewing the manuscripts. SC is supported by a Canada CIFAR AI Chair and an NSERC Discovery Grant.

REFERENCES

- Abien Fred Agarap. Deep learning using rectified linear units (relu). *arXiv*, 2018.
- Naman Agarwal, Brian Bullins, Xinyi Chen, Elad Hazan, Karan Singh, Cyril Zhang, and Yi Zhang. Efficient full-matrix adaptive regularization. In *International Conference on Machine Learning*, pages 102–110. PMLR, 2019.
- Zeyuan Allen-Zhu and Yang Yuan. Improved svrg for non-strongly-convex or sum-of-non-convex objectives. In *International conference on machine learning*, pages 1080–1089. PMLR, 2016.
- Marcin Andrychowicz, Misha Denil, Sergio Gómez Colmenarejo, Matthew W Hoffman, David Pfau, Tom Schaul, Brendan Shillingford, and Nando de Freitas. Learning to learn by gradient descent by gradient descent. In *NeurIPS*, 2016.
- Mahmoud Assran and Michael Rabbat. On the convergence of nesterov’s accelerated gradient method in stochastic settings. *arXiv preprint arXiv:2002.12414*, 2020.
- Emmanuel Bengio, Joelle Pineau, and Doina Precup. Correcting momentum in temporal difference learning. *Deep Learning Workshop, NeurIPS*, 2020.
- Léon Bottou. On-line learning and stochastic approximations. *On-Line Learning in Neural Networks*, 1999.
- Léon Bottou, Frank E Curtis, and Jorge Nocedal. Optimization methods for large-scale machine learning. *Siam Review*, 60(2):223–311, 2018.
- Samuel R. Bowman, Gabor Angeli, Christopher Potts, and Christopher D. Manning. A large annotated corpus for learning natural language inference. In *Proceedings of the 2015 Conference on Empirical Methods in Natural Language Processing*, pages 632–642, Lisbon, Portugal, September 2015. Association for Computational Linguistics. doi: 10.18653/v1/D15-1075. URL <https://www.aclweb.org/anthology/D15-1075>.
- Sébastien Bubeck. Convex optimization: Algorithms and complexity. *Foundations and Trends in Machine Learning*, 8(3-4):231–357, 2015.
- Paweł Budzianowski, Tsung-Hsien Wen, Bo-Hsiang Tseng, Inigo Casanueva, Stefan Ultes, Osman Ramadan, and Milica Gašić. Multiwoz—a large-scale multi-domain wizard-of-oz dataset for task-oriented dialogue modelling. In *EMNLP*, 2018.
- Aaron Defazio, Francis Bach, and Simon Lacoste-Julien. Saga: A fast incremental gradient method with support for non-strongly convex composite objectives. In *NeurIPS*, 2014.
- Dheeru Dua and Casey Graff. UCI machine learning repository, 2017.
- John Duchi, Elad Hazan, and Yoram Singer. Adaptive subgradient methods for online learning and stochastic optimization. *JMLR*, 2011.
- Nidham Gazagnadou, Robert Gower, and Joseph Salmon. Optimal mini-batch and step sizes for SAGA. In *ICML*, 2019.
- Saeed Ghadimi and Guanghui Lan. Accelerated gradient methods for nonconvex nonlinear and stochastic programming. *Mathematical Programming*, 156(1-2):59–99, 2016.
- Alex Graves, Greg Wayne, and Ivo Danihelka. Neural turing machines. *arXiv*, 2014.
- Alex Graves, Greg Wayne, Malcolm Reynolds, Tim Harley, Ivo Danihelka, Agnieszka Grabska-Barwińska, Sergio Gómez Colmenarejo, Edward Grefenstette, Tiago Ramalho, John Agapiou, et al. Hybrid computing using a neural network with dynamic external memory. *Nature*, 2016.
- Caglar Gulcehre, Sarath Chandar, Kyunghyun Cho, and Yoshua Bengio. Dynamic neural turing machine with continuous and discrete addressing schemes. *Neural computation*, 2018.
- Geoffrey Hinton, Nitish Srivastava, and Kevin Swersky. Neural networks for machine learning lecture 6a overview of mini-batch gradient descent, 2012.

- Sepp Hochreiter and Jürgen Schmidhuber. Long short-term memory. *Neural Computation*, 1997.
- Bin Hu and Laurent Lessard. Dissipativity theory for nesterov’s accelerated method. In *International Conference on Machine Learning*, pages 1549–1557. PMLR, 2017.
- Sashank J. Reddi, Ahmed Hefny, Suvrit Sra, Barnabas Póczos, and Alexander J Smola. On variance reduction in stochastic gradient descent and its asynchronous variants. In *NeurIPS*, 2015.
- Rie Johnson and Tong Zhang. Accelerating stochastic gradient descent using predictive variance reduction. In *NeurIPS*, 2013.
- Diederik P. Kingma and Jimmy Ba. Adam: A method for stochastic optimization. In Yoshua Bengio and Yann LeCun, editors, *ICLR*, 2015.
- Alex Krizhevsky, Geoffrey Hinton, et al. Learning multiple layers of features from tiny images. In *Citeseer*, 2009.
- Yann LeCun and Corinna Cortes. MNIST handwritten digit database. <http://yann.lecun.com/exdb/mnist/>, 2010. URL <http://yann.lecun.com/exdb/mnist/>.
- Yann LeCun, Patrick Haffner, Léon Bottou, and Yoshua Bengio. Object recognition with gradient-based learning. In *Shape, contour and grouping in computer vision*. Springer, 1999.
- Laurent Lessard, Benjamin Recht, and Andrew Packard. Analysis and design of optimization algorithms via integral quadratic constraints. *SIAM Journal on Optimization*, 26(1):57–95, 2016.
- David D. Lewis, Yiming Yang, Tony G. Rose, and Fan Li. Rcv1: A new benchmark collection for text categorization research. *JMLR*, 2004.
- Ke Li and Jitendra Malik. Learning to optimize. In *ICLR*, 2017.
- Yinhan Liu, Myle Ott, Naman Goyal, Jingfei Du, Mandar Joshi, Danqi Chen, Omer Levy, Mike Lewis, Luke Zettlemoyer, and Veselin Stoyanov. Roberta: A robustly optimized bert pretraining approach. *arXiv*, 2019.
- Mitchell P. Marcus, Mary Ann Marcinkiewicz, and Beatrice Santorini. Building a large annotated corpus of english: The penn treebank. *Computational Linguistics*, 1993.
- Stephen Merity, Caiming Xiong, James Bradbury, and Richard Socher. Pointer sentinel mixture models. *arXiv preprint arXiv:1609.07843*, 2016.
- Luke Metz, Niru Maheswaranathan, C. Daniel Freeman, Ben Poole, and Jascha Sohl-Dickstein. Tasks, stability, architecture, and compute: Training more effective learned optimizers, and using them to train themselves. *arXiv*, 2020.
- Aryan Mokhtari, Alej, and ro Ribeiro. Global convergence of online limited memory bfgs. *Journal of Machine Learning Research*, 2015.
- Y. E. Nesterov. A method for solving the convex programming problem with convergence rate $o(1/k^2)$. *Dokl. Akad. Nauk SSSR*, 1983.
- Yurii Nesterov. Introductory lectures on convex optimization: a basic course. *Kluwer Academic Publishers*, pages 71–81, 2004.
- Lam M. Nguyen, Jie Liu, Katya Scheinberg, and Martin Takáč. SARAH: A novel method for machine learning problems using stochastic recursive gradient. In *ICML*, 2017.
- Jorge Nocedal. Updating quasi-newton matrices with limited storage. *Mathematics of Computation*, 1980.
- Mansheej Paul, Surya Ganguli, and Gintare Karolina Dziugaite. Deep learning on a data diet: Finding important examples early in training. *NeurIPS*, 2021.
- Boris T. Polyak. Some methods of speeding up the convergence of iteration methods. *USSR Computational Mathematics and Mathematical Physics*, 4(5):1–17, 1964a.

- B.T. Polyak. Some methods of speeding up the convergence of iteration methods. *USSR Computational Mathematics and Mathematical Physics*, 1964b.
- Herbert Robbins and Sutton Monro. A stochastic approximation method. *The Annals of Mathematical Statistics*, 1951.
- Nicolas Roux, Mark Schmidt, and Francis Bach. A stochastic gradient method with an exponential convergence rate for finite training sets. In *NeurIPS*, 2012.
- David E Rumelhart, Geoffrey E Hinton, and Ronald J Williams. Learning internal representations by error propagation. Technical report, California Univ San Diego La Jolla Inst for Cognitive Science, 1985.
- Nicol N. Schraudolph, Jin Yu, and Simon Günter. A stochastic quasi-newton method for online convex optimization. In *AISTATS*, 2007.
- Shai Shalev-Shwartz and Tong Zhang. Stochastic dual coordinate ascent methods for regularized loss minimization. *JMLR*, 2013.
- Nitish Srivastava, Geoffrey Hinton, Alex Krizhevsky, Ilya Sutskever, and Ruslan Salakhutdinov. Dropout: a simple way to prevent neural networks from overfitting. *JMLR*, 2014.
- Ilya Sutskever, James Martens, George Dahl, and Geoffrey Hinton. On the importance of initialization and momentum in deep learning. In *ICML*, 2013.
- Oriol Vinyals and Quoc Le. A neural conversational model. *arXiv*, 2015.
- Matthew D Zeiler. Adadelta: an adaptive learning rate method. *arXiv*, 2012.
- Dongruo Zhou, Pan Xu, and Quanquan Gu. Stochastic nested variance reduction for nonconvex optimization. *arXiv preprint arXiv:1806.07811*, 2018.

A GENERAL CRITICAL GRADIENT ALGORITHM

We present the pseudocode for the Critical Gradient algorithm below.

Algorithm 1 Critical Gradients Optimization

Define #epochs E , #gradient updates B , model θ , learning rate α
Define optimizer $O(g_t, \theta_t, \mathbf{h})$, which produces a parameter update given gradient g_t , parameter θ_t and hyperparameters \mathbf{h}
Define aggregation function $\text{aggr}(g_t, \mathbf{g}_c)$ which outputs a linear combination of g_t and the entries in \mathbf{g}_c
Initialize empty critical gradient buffer $\{\mathbf{g}_c\}$ with decay rate d
for $s = 0$ **to** E **do**
 for $t = 0$ **to** B **do**
 Sample an input-output pair (x_i, y_i)
 $g_t \leftarrow \nabla_{\theta} L_i(\theta_t)$
 $\theta_{t+1} \leftarrow O(\text{aggr}(g_t, \mathbf{g}_c), \theta_t, \mathbf{h})$
 if $\{\mathbf{g}_c\}$ is not full **then**
 Add g_t to $\{\mathbf{g}_c\}$
 else
 if $\|g_t\|_2 > \|\min(\{\mathbf{g}_c\})\|_2$ **then**
 Remove $\min(\{\mathbf{g}_c\})$ from $\{\mathbf{g}_c\}$
 Add g_t to $\{\mathbf{g}_c\}$
 end if
 end if
 for $g_c \in \{\mathbf{g}_c\}$ **do**
 $\|g_c\|_2 \leftarrow d \cdot \|g_c\|_2$
 end for
 end for
end for

B CONVERGENCE PROOF

Proof. Recall that if $F : \mathbb{R}^d \rightarrow R$ is twice continuously differentiable, then for all $x, y \in \mathbb{R}^d$

$$\nabla F(y) = \nabla F(x) + \int_0^1 \nabla^2 F(x + t(y-x)) dt (y-x). \quad (7)$$

Letting $r_k := \theta_k - \theta^*$ denote the suboptimality of the parameters at iteration k and applying (7) with $y = \theta_k$ and $x = \theta^*$, we get that

$$g_k = H_k r_k + \zeta_k, \quad \text{where} \quad H_k = \int_0^1 \nabla^2 f(\theta^* + t r_k) dt,$$

where ζ_k denotes the gradient noise at iteration k . Using this and bounded staleness assumption, we have that

$$\text{aggr}(g_t, \mathcal{G}_t) = \sum_{k=0}^{K-1} w_{t,k} g_{t-k} = \sum_{k=0}^{K-1} w_{t,k} (H_{t-k} r_{t-k} + \zeta_{t-k}), \quad (8)$$

where $\{w_{t,k}\}_{k=0}^{K-1}$ are non-negative scalars in the closed interval $[0, 1]$ used to linearly aggregate the gradients in memory with the most recent gradient g_t . For gradients g_{t-k} that are not stored in memory, the corresponding aggregation scalar $w_{t,k}$ is equal to 0. Without loss of generality, we take $w_{t,0} = 1$, since we can always incorporate it into the step-size α and re-scale the other weights $w_{t,1}, \dots, w_{t,K-1}$ accordingly. Substituting (8) into (1) and subtracting θ^* from each side, we get that

$$r_{t+1} = r_t - \alpha \sum_{k=0}^{K-1} w_{t,k} (H_{t-k} r_{t-k} + \zeta_{t-k}).$$

Thus, we have that SGD_C evolves according to the linear system

$$\begin{bmatrix} r_{t+1} \\ r_t \\ \vdots \\ r_{t+1-K} \end{bmatrix} = A_t \begin{bmatrix} r_t \\ r_{t-1} \\ \vdots \\ r_{t-K} \end{bmatrix} - \alpha \begin{bmatrix} \sum_{k=0}^{K-1} w_{t,k} \zeta_{t-k} \\ 0 \\ \vdots \\ 0 \end{bmatrix} \quad \text{where} \quad A_t = \begin{bmatrix} T_{t,0} & T_{t,1} & \cdots & T_{t,K-1} \\ 0 & I & \cdots & 0 \\ \vdots & \vdots & \ddots & \vdots \\ 0 & 0 & \cdots & I \end{bmatrix},$$

with $T_{t,0} = I - \alpha H_t$ and $T_{t,k} = -\alpha w_{t,k} H_{t-k}$ for $k = 1, \dots, K - 1$. Unrolling the recursion, we have that

$$\begin{bmatrix} r_{t+1} \\ r_t \\ \vdots \\ r_{t+1-K} \end{bmatrix} = (A_t \cdots A_1) \begin{bmatrix} \theta_1 - \theta^* \\ 0 \\ \vdots \\ 0 \end{bmatrix} - \alpha \begin{bmatrix} \sum_{k=0}^{K-1} w_{t,k} \zeta_{t-k} \\ 0 \\ \vdots \\ 0 \end{bmatrix} - \alpha \sum_{j=1}^{t-1} (A_t \cdots A_{j+1}) \begin{bmatrix} \sum_{k=0}^{K-1} w_{j,k} \zeta_{j-k} \\ 0 \\ \vdots \\ 0 \end{bmatrix}, \quad (9)$$

from which it is clear that we may expect convergence properties to depend on the spectral properties of the matrices $\{A_k\}_{k=1}^t$. The convergence rate of SGD_C will therefore depend on the largest singular value of the matrices $\{A_k\}_{k=1}^t$. From Polyak (1964a, Lemma 4), we have that

$$\|A_j\| \leq \sup_{\{w_k \in [0,1]\}, \{\eta_k \in [\mu, L]\}} \rho(\Lambda), \quad (10)$$

where $\rho(\Lambda)$ are the singular values of the numerical matrix

$$\Lambda := \begin{bmatrix} \lambda_0 & \lambda_1 & \cdots & \lambda_{K-1} \\ 0 & 1 & \cdots & 0 \\ \vdots & \vdots & \ddots & \vdots \\ 0 & 0 & \cdots & 1 \end{bmatrix} \in \mathbb{R}^{K \times K},$$

with $\lambda_0 = 1 - \alpha \eta_0$ and $\lambda_k = -\alpha w_k \eta_k$ for $k = 1, \dots, K - 1$. Note that Polyak (1964a, Lemma 4) originally refers to the eigenvalues of a block matrix, however, in the case where the blocks are commutative, it is straightforward to extend the lemma to describe the singular values. To see this, simply apply the original lemma to the eigenvalues of the matrix $\Lambda^\top \Lambda$, where commutativity of the individual blocks ($T_{j,0}, \dots, T_{j,K}$ are all symmetric and therefore commutative) allows you to specify the eigenvalues of the new block matrix in terms of the eigenvalues of the original blocks.

Letting $q_{(\alpha, K)}$ denote the right hand side of (10), we have that $\|A_j\| \leq q_{(\alpha, K)}$ for all $j = 1, \dots, t$, and $q_{(\alpha, K)}$ has an analytic definition as the roots of a polynomial. Taking 2-norms, applying submultiplicativity of matrix norms, and using the bounded variance assumption along with the fact that the noise terms $\{\zeta_k\}_{k=0}^t$ are mutually independent and that the aggregation weights $\{w_{t,k}\}_{t \geq 0, k \in [1, K]}$ are in the closed interval $[0, 1]$ for all t, k , we have that

$$\mathbb{E} \|r_{t+1}\|^2 \leq q_{(\alpha, K)}^{2t} \|\theta_1 - \theta^*\|^2 + \alpha^2 \sigma^2 K \sum_{j=1}^t q_{(\alpha, K)}^{2(t-j)}, \quad (11)$$

where the expectation on the left hand side is with respect to the joint distribution over the random noise variables ζ_k, \dots, ζ_1 .

By assumption, since the step-size α is chosen such that $q_{(\alpha, K)} < 1$, equation (11) simplifies as

$$\mathbb{E} \|r_{t+1}\|^2 \leq q_{(\alpha, K)}^{2t} \|\theta_1 - \theta^*\|^2 + \frac{\alpha^2 K}{1 - q_{(\alpha, K)}^2} \sigma^2,$$

where we have implicitly used the upper bound on the limit of a geometric sequence. \blacksquare

C DATA SET DISTRIBUTIONS

Table 1 details the train-valid-test splits of all the data sets used in the experiments.

Dataset	#Train	#Valid	#Test
covtype	5000	N/A	N/A
rev1	5000	N/A	N/A
MNIST	50K	10K	10K
CIFAR-10	40K	10K	10K
CIFAR-100	40K	10K	10K
SNLI	550K	10K	10K
WikiText	2M	213K	241K
Penn TreeBank	890K	70K	78K
MultiWoZ	115K (1.5M)	20K (200K)	20K (200K)

Table 1: The splits of the data sets in number of samples. For WikiText, Penn TreeBank and MultiWoZ as the models are trained on a language modeling objective, the splits are given in number of tokens. For MultiWoZ, the number of utterances is provided with the number of tokens in parentheses.

D EXPERIMENT DETAILS

We tested the proposed class of optimizers on different tasks that have potentially different loss surfaces in large parameter spaces. To cast a wide net and ensure that we capture a plethora of neural architectures, we vary the network designs by using fully-connected, recurrent (Rumelhart et al., 1985), convolutional (LeCun et al., 1999), dropout (Srivastava et al., 2014), ReLU (Agarap, 2018) layers and a large Transformer language model architecture – RoBERTa-Base (Liu et al., 2019) across different tasks. A brief description of the data and architectures used follows.

CIFAR-10 is an image classification task with 10 classes. We train a shallow Convolutional Neural Network (ConvNet) with dropout and ReLU activation using the different optimizers and their \mathcal{C} variants.

CIFAR-100 is an image dataset similar in size to CIFAR-10 but with 100 classes of images. This task was approached using a Convolutional Neural Network with three batch-normalized convolutional blocks and one fully-connected block with dropout applied between blocks.

We experiment with the commonly-used language inference dataset, Stanford Natural Language Inference (SNLI) dataset, to compare the performances of \mathcal{C} variants training on three different text encoder architectures: 4-layer convolutional network (ConvNetEncoder), 2 layer bi-directional encoder with 2 linear projection layers (InferSent) and a unidirectional LSTM with 2 recurrent layers (LSTMEncoder). The classifier on top of the representations learned by the encoder architectures is a 2-layer fully-connected Multi-Layer Perceptron with dropout connection.

The Penn Tree Bank (PTB) is a syntax-annotated text corpus sourced from stories from the Wall Street Journal. We use this corpus for a word-level language modeling task using a 1-layer LSTM with dropout. Gradient clipping is employed to avoid exploding gradients. We evaluate the model by measuring perplexity (PPL) in the validation set; lower PPL scores are preferred.

MultiWoZ 2.0 is a popular dataset that has human-to-human goal-oriented conversations on different topics. The objective is to generate the next utterance conditioned on the history of utterances in the conversation. We experiment with a very large language model architecture – RoBERTa-Base – and a BiLSTM Sequence-to-Sequence architecture (Vinyals and Le, 2015) for the next utterance prediction. RoBERTa was trained with CausalLM-Head while BiLSTM model was an encoder-decoder architecture with a Bi-LSTM encoder and LSTM with Attention decoder.

We use models with varying size of trainable parameters as shown in Table 2.

Table 2: We experimented with models with different sizes for a comprehensive study of the proposed \mathcal{C} variants.

Model	#Params	Dataset(s)
Logistic Regression	8K (55/64)	MNIST (rcv1/covtype)
NeuralNetwork	25K	MNIST
ConvNet	600K (62K)	CIFAR-100 (CIFAR-10)
LSTM	20K (600K)	PTB (WikiText)
LSTMEncoder	600K	SNLI
InferSent	1.2M	SNLI
ConvNetEncoder	3.1M	SNLI
RoBERTa-Base	125M	MultiWoZ
Bi-LSTM	574K	MultiWoZ

We use the same hyperparameter initialization for comparisons with base optimization methods and tune the learning rate hyperparameter using grid search. The primary objective of the experiments is to verify the consistency of convergence to better solutions across tasks and architectures. All reported results are averaged over 5 different runs with different random seed values.

D.1 MODEL HPARAMS

All experiments are averaged for 5 different runs with different seeds. We use PyTorch 1.1 for the experiments and use their implementation of the base optimizers available in `torch.optim`. The details of hyperparameters used for the model are in Table 3.

Table 3: Architecture details for models used in experiments.

Model	Dataset	#Layers	#Hidden	ReLU/Dropout
Log. Reg.	covtype	1	N/A	No/No
Log. Reg.	rc1	1	N/A	No/No
Log. Reg.	MNIST	1	N/A	No/No
Log. Reg.	synthetic	1	N/A	No/No
MLP	MNIST	2	32	Yes/No
CNN	CIFAR-10	5	120	Yes/Yes
CNN	CIFAR-100	9	4096	Yes/Yes
LSTM	PTB	1	128	No/No
LSTM	WikiText	1	128	No/No
ConvNetEnc.	SNLI	2	200	Yes/Yes
LSTMEncoder	SNLI	2	200	No/Yes
InferSent	SNLI	2	200	Yes/Yes
RoBERTa-Base	MultiWoZ	12	768	Yes/Yes
Bi-LSTM Attn	MultiWoZ	4	200	No/No

D.2 RUNTIME STATISTICS

We logged the approximate time for each epoch for different values of topC across the different models. Although the results are populated from the experiments with Adam and its C variants, the results can be extended to the other optimizers and its variants. These times are reported in Table 4.

Table 4: Approximate time taken for one epoch of training of the models in the public repositories on the different data sets. The time is clocked in minutes. The time per epoch increases linearly with increase in topC over the (B)ase method. Although for lower values of topC the time per epoch is smaller, there is still room for improvement to bring down the time with smart update rules as discussed in §7.

Dataset	Model	B	C5	C10	C20	C20	C100
MNIST	Log.Reg	0.3	0.4	0.5	0.6	0.9	.5
	Neural-Net	0.3	0.5	0.6	0.8	1.4	2.3
PTB	LSTM	0.08	0.4	0.6	0.9	2	6
WikiText	LSTM	0.6	1	1.4	2.6	5	10
CIFAR-10	CNN	0.5	0.9	1	1.5	3	5
CIFAR-100	CNN	0.75	1.5	2	4	6	12
	LSTMEnc.	1	3	6	10	25	45
SNLI	InferSent	2	4	9	20	35	50
	ConvNet	1	4	8	20	40	65
MultiWoZ	RoBERTa	15	25	35	50	NA	NA
	BiLSTM	3	4	5	5	7	10

E HYPERPARAMETERS

E.1 RANGE OF HPARAMS

We present the range of hyperparameters used in our experiments (Table 5). Optimizer-specific parameters were used on both their vanilla and C versions.

Table 5: The hyperparameter configurations of the different optimizers in the experiments.

Hparam	Choices
Adam β_1	{0.9, 0.99, 0.999}
Adam β_2	{0.99, 0.999, 0.9999}
RMSprop α	{0.9, 0.99, 0.999}
SGDM <i>momentum</i>	{0.9, 0.99, 0.999}
<i>learning_rate</i>	{0.1, 0.01, 0.001, 0.0001, 0.00001}
decay	{0.7, 0.9, 0.99}
topC	{5, 10, 20}

E.2 HPARAMS OF THE BEST CONFIGURATIONS

The learning rates and other hyperparameters of the optimizers used in the results reported in the paper are listed in Tables 6, 7, 8 and 9.

Table 6: Best hyperparameter configurations for CIFAR-10 and CIFAR-100 image classification tasks.

Dataset	Model	Optimizer	Learning Rate	topC	decay	Momentum	β_1	β_2	α
CIFAR-10	Shallow ConvNet	$Adam_C$	0.0001	5	0.7	N/A	0.99	0.99	N/A
		Adam	0.001	N/A	N/A	N/A	0.9	0.99	N/A
		$RMSprop_C$	0.0001	5	0.7	N/A	N/A	N/A	0.9
		RMSprop	0.0001	N/A	0	N/A	N/A	N/A	0.9
		$SGDM_C$	0.001	5	0.7	0.9	N/A	N/A	N/A
		SGDM	0.001	N/A	N/A	0.9	N/A	N/A	N/A
		SGD_C	0.01	5	0.99	N/A	N/A	N/A	N/A
		SGD	0.01	N/A	N/A	N/A	N/A	N/A	N/A
		CIFAR-100	Deep ConvNet	$Adam_C$	0.00001	20	0.7	N/A	0.9
Adam	0.0001			N/A	N/A	N/A	0.9	0.9999	N/A
$RMSprop_C$	0.00001			20	0.7	N/A	N/A	N/A	0.99
RMSprop	0.0001			N/A	N/A	N/A	N/A	N/A	0.99
$SGDM_C$	0.001			20	0.7	0.9	N/A	N/A	N/A
SGDM	0.01			N/A	N/A	0.9	N/A	N/A	N/A
SGD_C	0.01			5	0.9	N/A	N/A	N/A	N/A
SGD	0.1			N/A	N/A	N/A	N/A	N/A	N/A

Table 7: Best hyperparameter configurations for language modelling tasks on WikiText and PennTree-Bank datasets.

Dataset	Model	Optimizer	LR	topC	decay	Momentum	β_1	β_2	α
PTB	LSTM	$Adam_C$	0.0001	5	0.9	N/A	0.9	0.999	N/A
		Adam	0.0001	0	0	N/A	0.9	0.999	N/A
		$RMSprop_C$	0.0001	20	0.9	N/A	N/A	N/A	0.9
		RMSprop	0.0001	0	0	N/A	N/A	N/A	0.9
		$SGDM_C$	0.1	10	0.9	0.9	N/A	N/A	N/A
		SGDM	0.1	0	0	0.9	N/A	N/A	N/A
		$SGDM_C$	0.1	2	0.95	N/A	N/A	N/A	N/A
		SGD	0.1	0	0	N/A	N/A	N/A	N/A
		Wikitext	LSTM	$Adam_C$	0.0001	20	0.9	N/A	0.9
Adam	0.0001			0	0	N/A	0.9	0.9999	N/A
$RMSprop_C$	0.0001			20	0.9	N/A	N/A	N/A	0.9
RMSprop	0.0001			0	0	N/A	N/A	N/A	0.9
$SGDM_C$	0.1			10	0.9	0.9	N/A	N/A	N/A
SGDM	0.1			0	0	0.9	N/A	N/A	N/A
$SGDM_C$	0.1			2	0.95	N/A	N/A	N/A	N/A
SGD	0.1			0	0	N/A	N/A	N/A	N/A

Table 8: Best hyperparameter configurations for text generation for dialogue on MultiWoZ2.0 dataset.

Dataset	Model	Optimizer	LR	topC	decay	Momentum	β_1	β_2	α
MultiWoZ2.0	RoBERTa-Base	$Adam_C$	0.00001	5	0.7	N/A	0.99	0.999	N/A
		Adam	0.00001	0	0	N/A	0.99	0.999	N/A
		$RMSprop_C$	0.0001	5	0.7	N/A	N/A	N/A	0.99
		RMSprop	0.00001	0	0	N/A	N/A	N/A	0.99
		$SGDM_C$	0.01	5	0.7	0.9	N/A	N/A	N/A
		SGDM	0.01	0	0	0.9	N/A	N/A	N/A
		SGD_C	0.1	5	0.7	N/A	N/A	N/A	N/A
		SGD	0.1	0	0	N/A	N/A	N/A	N/A
		Bi-LSTM	$Adam_C$	0.001	5	0.7	N/A	0.99	0.999
	Adam		0.001	0	0	N/A	0.99	0.999	N/A
	$RMSprop_C$		0.001	5	0.7	N/A	N/A	N/A	0.99
	RMSprop		0.001	0	0	N/A	N/A	N/A	0.99
	$SGDM_C$		0.1	5	0.7	0.9	N/A	N/A	N/A
	SGDM		0.1	0	0	0.9	N/A	N/A	N/A
	SGD_C		0.1	5	0.7	N/A	N/A	N/A	N/A
	SGD		0.1	0	0	N/A	N/A	N/A	N/A

F ANALYSIS

F.1 NOTE ON AGGREGATION

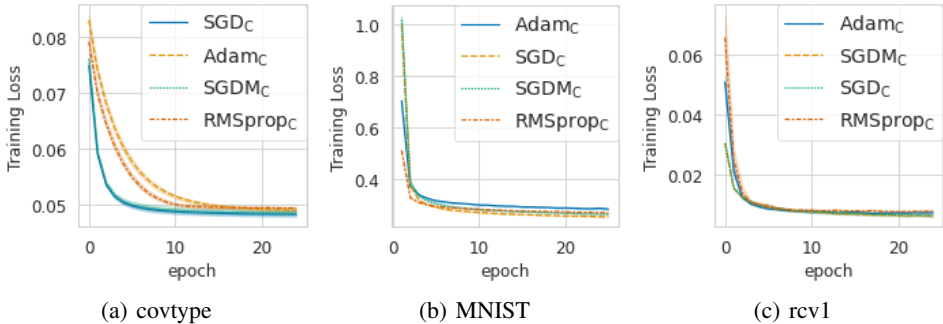
The aggregation function `aggr` lies at the core of integrating critical gradients into an algorithm. In §2 we presented `mean` and `sum` function for aggregation. The notable difference in these methods is the importance of the current gradient, as it is more heavily weighted with `sum` (which does not scale it) than with `mean` (which scales it by a factor of $\frac{1}{topC+1}$). While our algorithms converged

Table 9: Best hyperparameter configurations for text classification for language inference on SNLI dataset.

Dataset	Model	Optimizer	LR	topC	decay	Momentum	β_1	β_2	α
SNLI	InferSent	Adam _C	0.0001	5	0.7	N/A	0.99	0.999	N/A
		Adam	0.001	0	0	N/A	0.99	0.999	N/A
		RMSprop _C	0.0001	5	0.7	N/A	N/A	N/A	0.99
		RMSprop	0.001	0	0	N/A	N/A	N/A	0.99
		SGDM _C	0.01	5	0.7	0.9	N/A	N/A	N/A
		SGDM	0.1	0	0	0.9	N/A	N/A	N/A
		SGD _C	0.1	5	0.7	N/A	N/A	N/A	N/A
	SGD	0.1	0	0	N/A	N/A	N/A	N/A	
	ConvEncoder	Adam _C	0.0001	5	0.7	N/A	0.99	0.999	N/A
		Adam	0.001	0	0	N/A	0.99	0.999	N/A
		RMSprop _C	0.0001	5	0.7	N/A	N/A	N/A	0.99
		RMSprop	0.001	0	0	N/A	N/A	N/A	0.99
		SGDM _C	0.01	5	0.7	0.9	N/A	N/A	N/A
		SGDM	0.1	0	0	0.9	N/A	N/A	N/A
		SGD _C	0.1	5	0.7	N/A	N/A	N/A	N/A
	SGD	0.1	0	0	N/A	N/A	N/A	N/A	
	BLSTMEncoder	Adam _C	0.0001	5	0.7	N/A	0.99	0.999	N/A
		Adam	0.001	0	0	N/A	0.99	0.999	N/A
		RMSprop _C	0.0001	5	0.7	N/A	N/A	N/A	0.99
		RMSprop	0.001	0	0	N/A	N/A	N/A	0.99
		SGDM _C	0.01	5	0.7	0.9	N/A	N/A	N/A
		SGDM	0.1	0	0	0.9	N/A	N/A	N/A
		SGD _C	0.1	5	0.7	N/A	N/A	N/A	N/A
	SGD	0.1	0	0	N/A	N/A	N/A	N/A	

using both aggregation methods, we found that SGD_C and SGDM_C demonstrated better validation performance using `sum` whereas RMSprop_C and Adam_C performed better using `mean`. This is likely due to both RMSprop and Adam having adaptive learning rates, allowing them to be more robust to changes in the scaling of the gradients.

F.2 CONVERGENCE IN CONVEX TASKS

Figure 7: The training on the three different convex datasets show that the _C variants of the base optimizers empirically converge.

To empirically validate our proof of convergence for the proposed methods on convex loss surfaces, we train all _C optimizer variants on three tasks with Logistic Regression: ℓ_2 -regularized binary classification with *rcv1* (Lewis et al., 2004), ℓ_2 -regularized multi-class classification on *covtype* (Dua and Graff, 2017), and non-regularized multi-class classification on MNIST. Figure 7 shows training losses for all optimizers converging towards a minimal training loss.

F.3 BUFFER STALENESS BOUND

We present additional results demonstrating the boundedness of the staleness of stored gradients (Figure 8).

F.4 ADDITIONAL ABLATION EXPERIMENTS

We present additional side-by-side comparisons of optimizers in the vein of §6 (Figure 9).

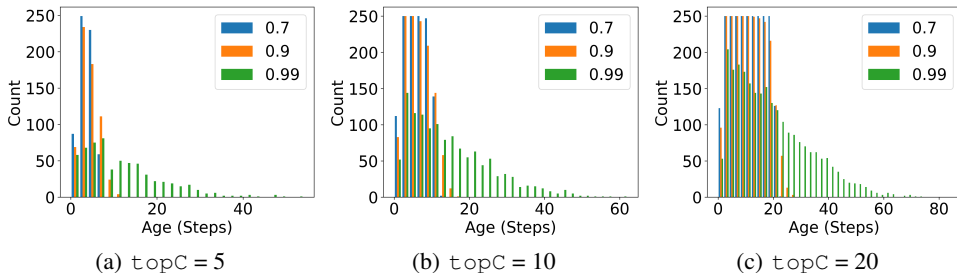


Figure 8: Histograms showing ages of the buffer as recorded at the end of every epoch, across five seeds, for Logistic Regression on MNIST.

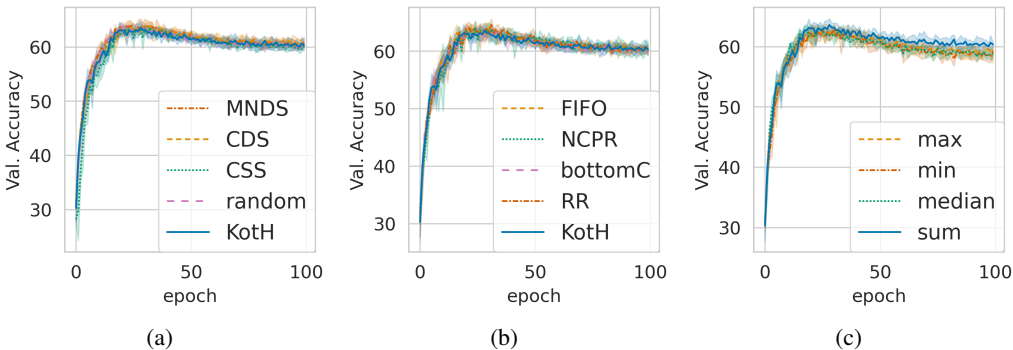


Figure 9: Additional ablation experiments performed on CIFAR-10

F.5 ROBUSTNESS TO NOISE

As C variants retain larger gradients during training, and noisy data points may have gradients with higher values of ℓ_2 -norm, we experiment with the C variants by training Logistic Regression on a synthetic binary classification dataset where the labels are perturbed with probability \mathcal{P}_{noise} .

We sample 500 data points from a 7-dimensional hypercube with the class means separated by 1 unit. The data is split by 80/20 for training and evaluation. We train the model with the optimizers for 20 epochs on a fixed learning rate of 1×10^{-3} , $\text{topC} = 5$, $\text{decay} = 0.5$ and other parameters from the base model set to their defaults.

We compare the performance of base method and its C variant to study anomalies when the C variants are exposed to noise (Figure 10). We observe that the models do not behave any differently than the base methods showcasing that the noise in the dataset does not affect the workings of the C variants even with a small value for topC . This could be attributed to the decay parameter of the optimizer that linearly scales down the priority of the older gradients in the buffer leading to them getting replaced.

To construct the synthetic data set for the experiments, we used sklearn’s `make_classification` method. The specific hyperparameters used to construct the dataset:

- `n_samples = 500, n_features = 10,`
- `n_informative=7, n_redundant=0, n_repeated=0,`
- `n_classes=2, n_clusters_per_class=1,`
- `weights=class_imbalance, flip_y=noise, class_sep= 0.5,`
- `hypercube=True, shift=0.4, scale=1.0, shuffle=True, random_state=1403`

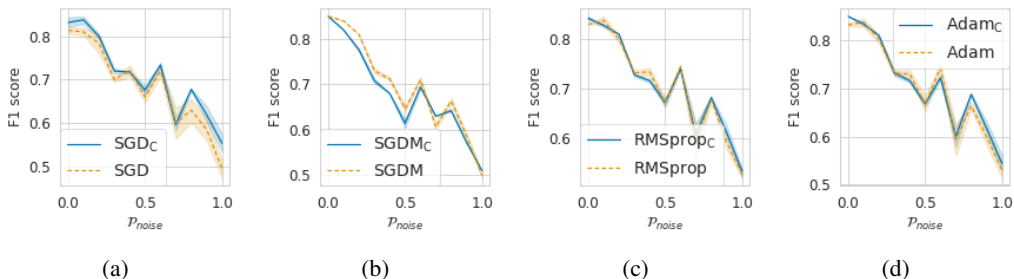


Figure 10: \mathcal{P}_{noise} is increased from 0 to 1 in increments of 0.1 indicating 10% more injection of noise. The proposed variants did not show any anomaly on a noise induced dataset. For the experiments on the decay the $topC$ was 5 and $decay$ 0.5. The plots are averaged over 5 different runs with different seeds.

F.6 DECAF

The optimizers’ sensitivity to decay (Figure 11) had similar trend in other experiments, where the optimizers showed better performance when decay was away from 0.99.

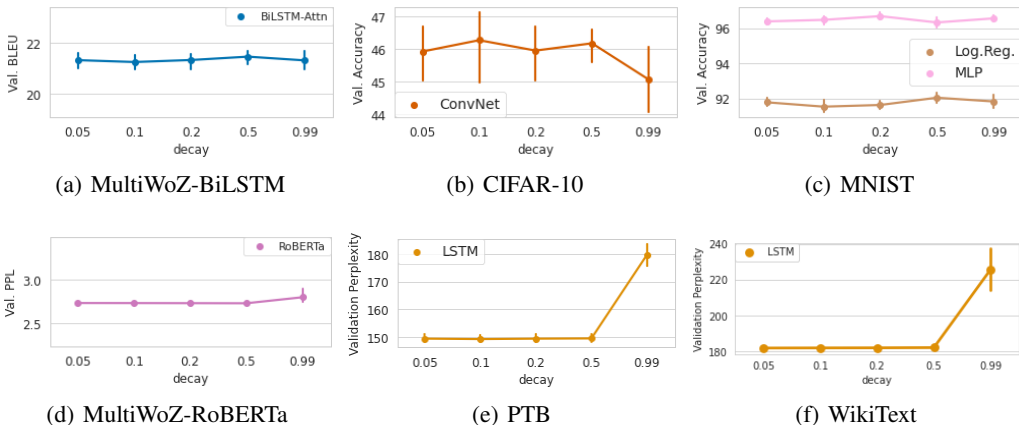


Figure 11: Experiments on varying decay that across tasks. Graphs in the top row measure BLEU score or accuracy (where a higher value is desired) and those in the bottom row measure perplexity (where a lower value is desired)

F.7 TOPC

The optimizers’ sensitivity to $topC$ (Figure 12) had a similar trend to other experiments, where the optimizers showed better performance for lower values of $topC$.

F.8 g_t VS g_c

As a follow-up experiment to validate the non-informative gradients with higher values of $topC$, we observe the trend in the difference between $average(\|g_c\|_2)$ and $\|g_t\|_2$ for different values of $topC$. We see that the gradients at each step get lower as $topC$ increases. This could be because of the stochasticity in $aggr$ when computed with fewer gradients, which incidentally allow models to converge better. Although storing all of the past gradients in memory has theoretical advantages, in practice we observe that lower $topC$ provides better training signal through g_c than g_t (Figure 13(a),13(b)). This explains the slightly lower performance of $topC = 100$ across models in SNLI task and the nonexistent to marginal improvements in MultiWoZ dataset with RoBERTa-Base model.

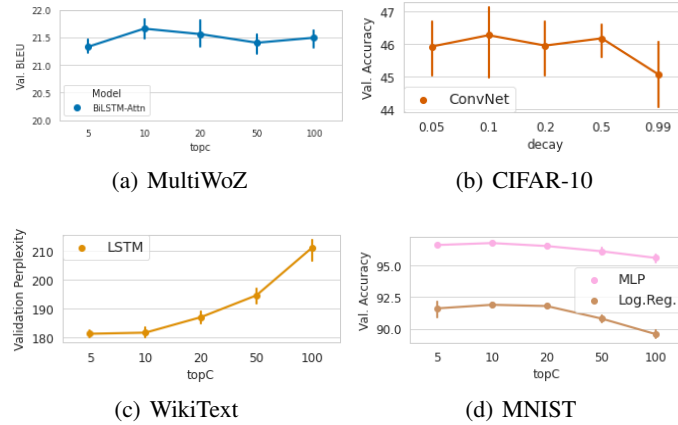


Figure 12: Experiments on varying topC that across tasks. Top row: (a) MultiWoz - BiLSTM (BLEU Score) (b) CIFAR-10 - Convnet (Accuracy). Bottom row: (c) WikiText - LSTM (Perplexity) (d) MNIST - Log. Reg. and MLP (Accuracy).

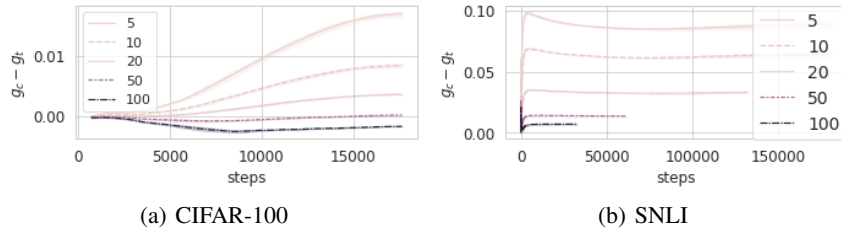


Figure 13: The difference between $\text{average}(\|g_c\|_2)$ and $\|g_t\|_2$ shown in plots (a) and (b) indicate that increasing topC could hurt the performance. These plots correlate to experiments in §6

The plots of g_t vs g_c is crucial to the results in that they provide an explanations for the faster convergence (as well as smaller improvements) of the C variants over the base methods (Figure 14). Since the parameter updates are reminded of large displacement of the gradients via the `aggr` method, the model updates the parameters more frequently. In the cases where g_c is higher than g_t , we observe better performance and no improvements in cases where the difference is not as significant.

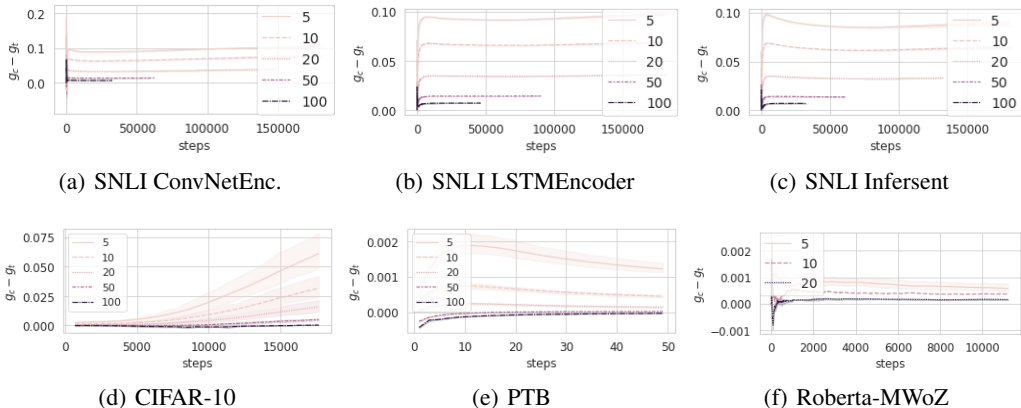


Figure 14: Additional results on g_t vs g_c , explaining rationale behind the better performances of lower values of `topC` across all the experiments. As the variance in `aggr` get diminished with increase in `topC` the model does not gain much with increase in `topC`.

Further, we observe the significance of the gradients as defined in ℓ_2 -norm diminishes as `topC` increases. This indicates that the optimizer needs only to store only a small set of critical gradients in order to improve the performance without incurring much time and memory overhead. Employing lazy updates to cut down on the time is a useful future direction of research.

F.9 DETAILS OF ABLATION EXPERIMENTS

We detail the various ablation experiments whose results are presented in §6.

- King of the Hill sampling: The default method for Critical Gradients. Incoming gradients are added if their norm is larger than the priority of the smallest gradient, which is subsequently removed.
- Smallest gradients (or "bottomC"): Replaces the max-heap buffer with a min-heap
- First-In-First-Out (FIFO): Replaces the max-heap (priority queue) buffer with a queue which begins to dequeue when it reaches a capacity of `topC`.
- "Coin-Toss"/"random": an incoming gradient is added to the buffer or not with equal probability.
- Mean-Norm Diversity Sampling (MNDS): Incoming gradients are probabilistically added to the buffer with likelihood proportional to its difference from the mean of the norms of gradients in the buffer.
- Cosine Diversity Sampling (CDS): Incoming gradients are probabilistically added to the buffer with likelihood *antiproportional* to its cosine similarity (normalized dot-product of flattened vectors).
- Cosine Similarity Sampling (CSS): Incoming gradients are probabilistically added to the buffer with likelihood *proportional* to its cosine similarity.
- Random Replacement (RR): When the buffer is full and a new gradient is added, the gradient which gets removed gets selected at random.

- Norm-Controlled Probabilistic Replacement (NCPR): When the buffer is full and a new gradient is added, the gradient g_k which gets removed gets selected with probability $\frac{\|g_k\|_2}{\sum_{g_i \in \mathbf{g}_c} \|g_i\|_2}$.

G TEST PERFORMANCE

The complete test performance of the models is reported in Table 10.

H REPRODUCIBILITY CHECKLIST

As per the prescribed Reproducibility Checklist, we provide the information of the following:

- *A clear description of the mathematical setting, algorithm and/or model:* We provide details of models used in §D
- *Submission of source code:* Source code for the proposed optimizers and its variants is provided as a zip. The code used to train the models on the different data sets are open source GitHub repositories. Other codes developed for the project are included in the zip.
- *Description of the computing infrastructure used:* We used 50 NVIDIA V100 32GB GPUs in parallel hyper parameter search over the grid using wandb and submitit packages. For the final runs we used 1 NVIDIA V100 32 GB GPUs for every seed of every model.
- *Average runtime for each approach:* The approximate training time for our use of Adam_C accross tasks is reported in §D.2.
- *Explanation of evaluation metrics used, with links to code:* The metrics used for evaluation of the models are the popular ones. For the ease of readers citations for the metrics are included in the paper.
- *Relevant statistics of the datasets used:* We provide the statistics of the datasets used in C.
- *Explanation of any data that were excluded, and all pre-processing steps:* We train on a fraction of the covtype and rcv1 datasets instead of using the entire data. We sampled 5000 datapoints at random with seed set to 100.
- *Link to downloadable version of data:* The data sets used in the paper are from public repositories. Links to the paper that proposes the data sets is included in the README.md files in the submitted repository.

Table 10: Complete test results on the different tasks.

Model	Dataset	Metric	Optimizer	Performance
RoBERTa	MWoZ	PPL	Adam	2.57 ± 0.0
RoBERTa	MWoZ	PPL	Adam _C	2.41 ± 0.0
RoBERTa	MWoZ	PPL	RMSprop	2.56 ± 0.01
RoBERTa	MWoZ	PPL	RMSprop _C	2.42 ± 0.0
RoBERTa	MWoZ	PPL	SGDM	2.46 ± 0.0
RoBERTa	MWoZ	PPL	SGDM _C	2.4 ± 0.01
RoBERTa	MWoZ	PPL	SGD	2.62 ± 0.01
RoBERTa	MWoZ	PPL	SGD _C	2.41 ± 0.0
Model	Dataset	Metric	Optimizer	Performance
BiLSTM	MWoZ	BLEU	Adam	20.64 ± 0.19
BiLSTM	MWoZ	BLEU	Adam _C	20.94 ± 0.26
BiLSTM	MWoZ	BLEU	RMSprop	21.3 ± 0.41
BiLSTM	MWoZ	BLEU	RMSprop _C	21.21 ± 0.22
BiLSTM	MWoZ	BLEU	SGDM	19.31 ± 0.27
BiLSTM	MWoZ	BLEU	SGDM _C	19.58 ± 0.47
BiLSTM	MWoZ	BLEU	SGD	14.26 ± 0.61
BiLSTM	MWoZ	BLEU	SGD _C	16.35 ± 0.24
Model	Dataset	Metric	Optimizer	Performance
LSTM	PTB	PPL	Adam	153.54 ± 1.65
LSTM	PTB	PPL	Adam _C	133.28 ± 0.61
LSTM	PTB	PPL	RMSprop	141.83 ± 0.57
LSTM	PTB	PPL	RMSprop _C	130.63 ± 0.64
LSTM	PTB	PPL	SGDM	139.93 ± 0.64
LSTM	PTB	PPL	SGDM _C	132.22 ± 1.1
LSTM	PTB	PPL	SGD	386.57 ± 18.61
LSTM	PTB	PPL	SGD _C	295.33 ± 2.96
Model	Dataset	Metric	Optimizer	Performance
LSTM	WikiText	PPL	Adam	170.3 ± 1.23
LSTM	WikiText	PPL	Adam _C	169.23 ± 1.06
LSTM	WikiText	PPL	RMSprop	180.42 ± 1.64
LSTM	WikiText	PPL	RMSprop _C	172.15 ± 1.63
LSTM	WikiText	PPL	SGDM	166.82 ± 2.24
LSTM	WikiText	PPL	SGDM _C	156.75 ± 1.32
LSTM	WikiText	PPL	SGD	461.84 ± 12.68
LSTM	WikiText	PPL	SGD _C	356.88 ± 8.34
Model	Dataset	Metric	Optimizer	Performance
InferSent	SNLI	Accuracy	Adam	78.42 ± 0.26
InferSent	SNLI	Accuracy	Adam _C	79.03 ± 0.18
InferSent	SNLI	Accuracy	RMSprop	77.91 ± 0.35
InferSent	SNLI	Accuracy	RMSprop _C	79.07 ± 0.28
InferSent	SNLI	Accuracy	SGDM	79.15 ± 0.3
InferSent	SNLI	Accuracy	SGDM _C	78.52 ± 0.26
InferSent	SNLI	Accuracy	SGD	78.3 ± 0.16
InferSent	SNLI	Accuracy	SGD _C	78.9 ± 0.57
Model	Dataset	Metric	Optimizer	Performance
ConvNet	SNLI	Accuracy	Adam	75.52 ± 0.0
ConvNet	SNLI	Accuracy	Adam _C	77.77 ± 0.28
ConvNet	SNLI	Accuracy	RMSprop	74.69 ± 0.36
ConvNet	SNLI	Accuracy	RMSprop _C	77.49 ± 0.24
ConvNet	SNLI	Accuracy	SGDM	76.79 ± 0.68
ConvNet	SNLI	Accuracy	SGDM _C	78.06 ± 0.45
ConvNet	SNLI	Accuracy	SGD	78.5 ± 0.1
ConvNet	SNLI	Accuracy	SGD _C	78.59 ± 0.24
Model	Dataset	Metric	Optimizer	Performance
LSTMEnc	SNLI	Accuracy	Adam	76.79 ± 0.38
LSTMEnc	SNLI	Accuracy	Adam _C	77.3 ± 0.09
LSTMEnc	SNLI	Accuracy	RMSprop	76.37 ± 0.36
LSTMEnc	SNLI	Accuracy	RMSprop _C	77.48 ± 0.11
LSTMEnc	SNLI	Accuracy	SGDM	77.6 ± 0.22
LSTMEnc	SNLI	Accuracy	SGDM _C	76.69 ± 1.04
LSTMEnc	SNLI	Accuracy	SGD	74.92 ± 1.32
LSTMEnc	SNLI	Accuracy	SGD _C	76.81 ± 0.59
Model	Dataset	Metric	Optimizer	Performance
ConvNet	CIFAR100	Accuracy	Adam	54.71 ± 0.55
ConvNet	CIFAR100	Accuracy	Adam _C	53.55 ± 0.42
ConvNet	CIFAR100	Accuracy	RMSprop	54.35 ± 0.5
ConvNet	CIFAR100	Accuracy	RMSprop _C	52.93 ± 0.57
ConvNet	CIFAR100	Accuracy	SGDM	56.03 ± 0.49
ConvNet	CIFAR100	Accuracy	SGDM _C	59.07 ± 0.2
ConvNet	CIFAR100	Accuracy	SGD	55.37 ± 0.39
ConvNet	CIFAR100	Accuracy	SGD _C	58.0 ± 0.37
Model	Dataset	Metric	Optimizer	Performance
ConvNet	CIFAR10	Accuracy	Adam	64.26 ± 0.47
ConvNet	CIFAR10	Accuracy	Adam _C	63.72 ± 0.37
ConvNet	CIFAR10	Accuracy	RMSprop	63.9 ± 0.33
ConvNet	CIFAR10	Accuracy	RMSprop _C	64.02 ± 0.78
ConvNet	CIFAR10	Accuracy	SGDM	64.7 ± 0.69
ConvNet	CIFAR10	Accuracy	SGDM _C	63.68 ± 0.77
ConvNet	CIFAR10	Accuracy	SGD	63.9 ± 0.63
ConvNet	CIFAR10	Accuracy	SGD _C	64.89 ± 0.66